Z. Phys. C 74, 509–515 (1997)

ZEITSCHRIFT
FÜR PHYSIK C

Properties of HERA events from DIS on pions in the proton

M. Przybycień[1,⋆], A. Szczurek[2], G. Ingelman[3,4]

[1] Faculty of Physics and Nuclear Techniques, Academy of Mining and Metallurgy, Al. Mickiewicza 30, PL-30-059 Cracow, Poland
[2] Institute of Nuclear Physics, ul.Radzikowskiego 152, PL-31-342 Cracow, Poland
[3] Deutsches Elektronen-Synchrotron DESY, Notkestrasse 85, D-22603 Hamburg, FRG
[4] Dept. of Radiation Sciences, Uppsala University, Box 535, S-751 21 Uppsala, Sweden

Received: 14 May 1996

Abstract. Recently the concept of the pion cloud in the nucleon turned out to be successful in understanding the Gottfried sum rule violation observed by the New Muon Collaboration and the Drell–Yan asymmetry measured in NA51 at CERN. We propose a further possibility to test this concept at HERA through the analysis of the structure of deep inelastic scattering (DIS) events induced by pion–exchange. Momentum and energy distributions of outgoing nucleons as well as rapidity and multiplicity distributions are investigated using Monte Carlo simulations. Most observables cannot distinguish this process from ordinary DIS, but in the energy distribution of final neutrons we find a significantly different prediction from the pion cloud model. Forward neutron calorimeters will be essential to test the concept of pions in the nucleon.

1 Introduction

In deep inelastic scattering (DIS) the incident lepton is scattered on a coloured quark. Normally this results in a colour field between the struck quark and the proton remnant, such that hadrons are produced in the whole rapidity region in between. In electron-proton collisions at HERA, this leads to particles being produced also close to the proton beam direction. The recent discovery by the ZEUS [1] and H1 [2] collaborations at HERA of large rapidity gap events has attracted much interest. This new class of DIS events have a large region of forward rapidity (i.e. close to the proton beam) where no particles or energy depositions are observed. The most forward hadronic activity being observed is then actually in the central part of the detectors. These large rapidity gap events cannot be described by standard models for DIS and hadronization [3, 4, 5]. Therefore the observation of a surprisingly large fraction ($\sim 10\%$) of events with a large rapidity gap strongly suggests the presence of a final proton close to the beam momentum. These events have, therefore, been primarily interpreted in terms of pomeron exchange (although alternative models have recently been proposed [6]).

In this interpretation, the lepton interacts with a colorless object having the quantum numbers of the vacuum, i.e. the pomeron. The experimental signature is then a quasi-elastically scattered proton well separated in rapidity from the other produced particles. The leading proton escapes undetected by the main detector, but may be observed in leading proton spectrometers that are coming into operation in both ZEUS and H1.

In the last few years, experiments on DIS have demonstrated that the internal structure of the nucleon is more complicated than expected. The polarized DIS experiments performed by EMC and SMC at CERN have shown that only a small fraction of the proton spin is carried by the valence quarks [7]. In addition, the strong violation of the Gottfried sum rule observed by NMC [8] strongly suggests a $d - \overline{u}$ asymmetry of the nucleon sea. The new fits of the parton distributions [9] to the world deep inelastic and Drell–Yan data (including the dedicated NA51 experiment [10]) seem to confirm the asymmetry. Both the violation of the Gottfried sum rule and the asymmetry measured in the Drell–Yan processes can be naturally accounted for by the presence of pions in the nucleon, as formulated in the pion cloud model [11]. In view of these successes of the pion cloud model, it is mandatory to consider its role in other phenomena.

The presence of such pions leads to an additional mechanism for nucleon production in DIS. In fixed target experiments, as (anti)neutrino deep inelastic scattering [12] for instance, it leads to the production of slow protons. The pion–exchange model describes the proton production on a neutron target [13] (extracted from deuteron data [14] obtained in bubble chamber experiments at CERN). With HERA kinematics the pion cloud induced mechanism leads to the production of rather fast forward protons and neutrons. The mechanism is shown schematically in Fig. 1. The virtual photon ‘smashes’ the virtual colorless pion into debris and the nucleon (proton or neutron) or an isobar is produced as a spectator of the reaction. In this respect there is full analogy to the reaction on the pomeron. Therefore, the pion cloud induced mechanism could also lead to rapidity gap events. In this paper, we investigate this processes and present quan-

⋆ supported by the Polish State Committee for Scientific Research, grant No.2P03B 244 08p02

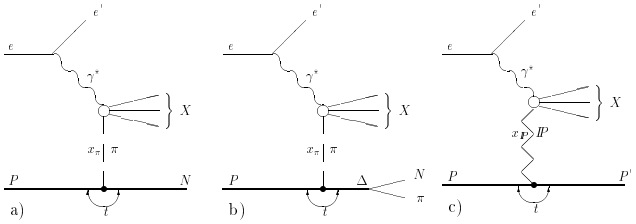

Fig. 1. Fast forward nucleon production at HERA: **(a)** direct production through pion-exchange, **(b)** indirect production via a Δ resonance in pion-exchange, **(c)** pomeron-exchange

titative results, not previously available in the literature.

To understand these processes, not only protons but also neutrons in the forward directions are interesting [15, 16]. Recently the ZEUS collaboration has installed a forward neutron calorimeter (FNCAL) [17] which will provide additional experimental information. In analogy to the hadronic reaction $pp \to nX$, the pion-exchange is expected to be the dominant mechanism of the fast neutron production also at HERA [15, 16]. Thus, HERA open new possibilities to test the concept of pion exchange and the pionic structure in the nucleon.

In the present paper we study several quantities which could be analyzed in HERA experiments; in particular using the main calorimeter, the leading proton spectrometer [18] (LPS) and the forward neutron calorimeter [17] in ZEUS. The main aim of the study is to find the best signal to identify the discussed mechanism of scattering on a pion in the proton.

2 Pion–exchange mechanism of fast nucleon production

In the meson cloud model [19] the nucleon is viewed as a quark core (called a bare nucleon) accompanied by the mesonic cloud. Restricting to the most important πN component, the Fock state decomposition of the light-cone proton is

$$|p\rangle = \sqrt{Z}\Big[|(3q)\rangle + \int dy\, d^2\mathbf{k}_T \phi(z,\mathbf{p}_T)$$

$$\times\Big(\sqrt{\frac{1}{3}}|p\pi^0, z, \mathbf{p}_T\rangle + \sqrt{\frac{2}{3}}|n\pi^+, z, \mathbf{p}_T\rangle\Big) + \ldots\Big], \qquad (1)$$

with Z being the wave function renormalization constant which can be calculated by imposing the normalization condition $\langle p|p\rangle = 1$. $\phi(z,\mathbf{p}_T)$ is the light cone wave function of the πN Fock state, where z is the longitudinal momentum fraction of the bare nucleon and $\mathbf{p}_T$ its transverse momentum.

The presence of virtual pions in the nucleon leads to an additional mechanism for nucleon production referred to as 'direct spectator' (Fig. 1a) and 'sequential spectator' (Fig. 1b) processes. The pion in the nucleon interacts with a virtual γ producing a system X. For comparison we show the pomeron-exchange mechanism in Fig. 1c. The cross section for the semi-inclusive spectator process $ep \to e'NX$ can be written as

$$\frac{d^4\sigma^{\rm sp}\big(ep \to e'NX\big)}{dx dQ^2 dz dp_T^2} =$$

$$\frac{1}{z} f_{\pi N}(1-z,t) \frac{d\sigma^{e\pi}(x/(1-z))}{d(x/(1-z))\, dQ^2}\ . \qquad (2)$$

The presence of the $\pi\Delta$ Fock component in the proton leads to the production of a spectator Δ which decays into a pion and a nucleon. The one–pion exchange contribution to the inclusive cross section can be obtained by integrating over unmeasured quantities

$$\frac{d\sigma^{ep}(x,Q^2)}{dx\, dQ^2} = \int_0^{1-x} dz \int_{-\infty}^{t(0,z)} dt\ f_{\pi N}(1-z,t)$$

$$\times \frac{d\sigma^{e\pi}(x/(1-z),Q^2)}{d(x/(1-z))\, dQ^2}, \qquad (3)$$

where $\sigma^{e\pi}$ is the cross section for the inclusive deep inelastic scattering of the electron from the virtual pion. In practical calculations the on-mass-shell $e\pi$ cross section can be used.

The probability density to find a meson with light–cone momentum fraction $x_\pi = (1-z)$ and four–momentum squared t (or alternatively transverse momentum $p_T^2 = -t(1-x_\pi) - m^2 x_\pi^2$) is referred to as the splitting function, which quantifies the presence of virtual mesons in the nucleon. The splitting function $f(x_\pi,t)$ to the πN Fock state (Fig. 1a) is

$$f_{\pi N}(x_\pi,t) = \frac{3g^2_{p\pi^0 p}}{16\pi^2} x_\pi \frac{(-t)|F_{\pi N}(x_\pi,t)|^2}{(t-m_\pi^2)^2}, \qquad (4)$$

and to the $\pi\Delta$ Fock state (Fig. 1b) is

$$f_{\pi\Delta}(x_\pi,t) =$$

$$\frac{2g^2_{p\pi^-\Delta^{++}}}{16\pi^2} x_\pi \frac{(M_+^2-t)^2(M_-^2-t)|F_{\pi\Delta}(x_\pi,t)|^2}{6m_N^2 m_\Delta^2 (t-m_\pi^2)^2}, \qquad (5)$$

where $M_+ = m_\Delta + m_N$ and $M_- = m_\Delta - m_N$. The couplings g^2 depend on the process, but via the isospin relations $g^2_{p\to\pi^+ n} : g^2_{p\to\pi^0 p} = 2:1$ and $g^2_{p\to\pi^+\Delta^0} : g^2_{p\to\pi^0\Delta^+} : g^2_{p\to\pi^-\Delta^{++}} = 1:2:3$ there are only two independent couplings which we take as $g^2_{p\to\pi^0 p}/4\pi = 13.6$ [20] and $g^2_{p\to\pi^-\Delta^{++}}/4\pi = 12.3$ GeV^{-2} [21]. The $F_{MB}(x_\pi,t)$ are vertex form factors, which account for the extended nature of the hadrons involved. The form factors used in meson exchange models are usually taken to be functions of t only. As discussed in [19] such form factors are a source of momentum sum rule violation and it was therefore suggested to use form factors which are functions of the invariant mass of the intermediate meson-baryon system, i.e. $M^2_{MB}(x_\pi,p_T^2) = \frac{m_\pi^2+p_T^2}{x_\pi} + \frac{m_B^2+p_T^2}{1-x_\pi}$.

It can be shown that such a vertex function arises naturally if one computes the splitting function $f(x_\pi,t)$ in time-ordered perturbation theory in the infinite momentum frame [22]. This functional form is typical for parameterizing the light-cone wave function of composed systems (see e.g. [23]).

In all calculations discussed below the vertex form factors have been assumed in the exponential form

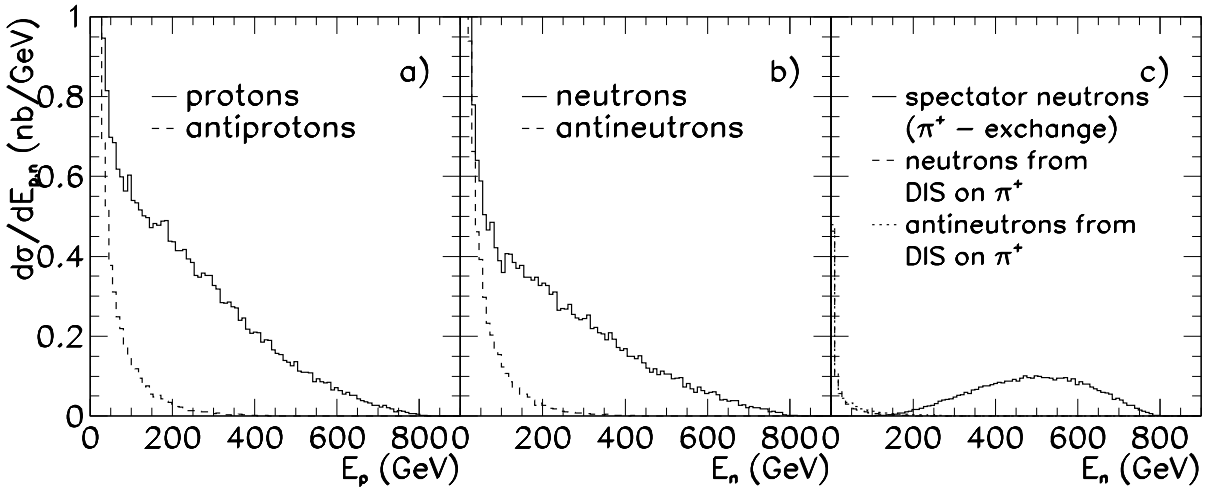

Fig. 2. Energy spectra in the HERA lab frame for nucleons ($p, \bar{p}, n, \bar{n}$) from **(a,b)** conventional DIS on a proton (obtained with LEPTO) and **(c)** DIS on an exchanged π^+ (obtained with POMPYT)

$$F_{MB}(x_\pi, p_T^2) = \exp\left[-\frac{M_{MB}^2(x_\pi, p_T^2) - m_N^2}{2\Lambda_{MB}^2}\right]. \quad (6)$$

By using the kinematical relation [24]

$$t = \frac{-p_T^2}{1-x_\pi} - x_\pi\left(\frac{m_B^2}{1-x_\pi} - m_N^2\right) \quad (7)$$

the form factor given by (6) can be equivalently expressed in terms of x_π and t in the simple form:

$$F_{MB}(x_\pi, t) = \exp\left[-\frac{m_\pi^2 - t}{2\Lambda_{MB}^2 x_\pi}\right]. \quad (8)$$

The cut-off parameters used in the present calculation ($\Lambda_{\pi N}$ = 1.10 GeV and $\Lambda_{\pi\Delta}$ = 0.98 GeV) have been determined from the analysis of the particle spectra for high-energy neutron and Δ production [19], i.e. $pp \to nX$ and $pp \to \Delta^{++}X$. With these cut-off parameters the NMC result for the Gottfried sum rule [8] which depends sensitively on Λ_{MB}, has been reproduced [19]. Furthermore the model describes the $\overline{u} - \overline{d}$ asymmetry extracted recently from the Drell-Yan experiment NA51 at CERN [25]. We note, however, that all results of this paper would be quite similar if traditional dipole form factors with cut-off parameter of 1.0–1.2 GeV had been used instead of (6).

In hadronic reactions quite often the Regge approach was used rather than the light–cone approach. In order to obtain the flux factor in the Regge approach it is sufficient to replace in (4) x_π by $x_\pi^{1-2\alpha_\pi(t)}$, where the pion's Regge trajectory $\alpha_\pi(t) = \alpha_\pi'(t - m_\pi^2)$. The reggeization is important for small x_π and/or large t. This is a kinematical region where the flux factor, especially with the vertex form factor (6), is rather small. Furthermore in the Regge approach, in contrast to the light–cone approach, it is not clear whether it would be fully consistent in the lepton DIS to use the on–shell pion structure function. However, since the difference is important only in very limited region of the phase space, in practice both approches lead to almost identical flux factors.

3 Results and discussion

The formalism presented above has been implemented in the Monte Carlo program POMPYT version 2.3 [26]. This program, which was originally for diffractive interactions via pomeron exchange, simulates the interaction dynamics resulting in the complete final state of particles. The basic hard scattering and perturbative QCD parton emission processes are treated based on the program PYTHIA [27] and the subsequent hadronization is according to the Lund string model [4] in its Monte Carlo implementation JETSET [27] which also handles particle decays.

The main difference in comparison to the pomeron case is the replacement of the pomeron flux factor by the pion flux factors given by (4,5) and the pomeron structure function by the pion structure function. The pion case is better contrained than the pomeron case, due to the better known pion structure function where those for the on-shell pion can be used. The pion parton densities from the parametrisation GRV-P HO ($\overline{MS}$) [28] is therefore used. It is important to mention in this context that the absolute normalization of the cross section for the production of the spectator nucleon via pion-exchange mechanism depends on the absolute value of the pion structure function. At the small-x relevant at HERA, the structure function is completely dominated by the pion sea contribution which is not very well known. Experimentally the pion structure function can be determined from the Drell–Yan processes only for $x > 0.1$ [29, 30]. If the pion-exchange mechanism is the dominant mechanism of fast neutron production, the coincidence measurement of scattered electrons and forward neutrons may allow the determination of the pion deep inelastic structure function [16]. When considering the event structure, however, the precise value of F_2^π is not required.

When the deep inelastic scattering is on a valence quark (antiquark) the pion remnant is simply the remaining antiquark (quark). A colour triplet string is then stretched between them and hadronization described with the Lund string model [4]. In case it is a sea quark (antiquark) that was struck, the pion remnant contains the associated sea

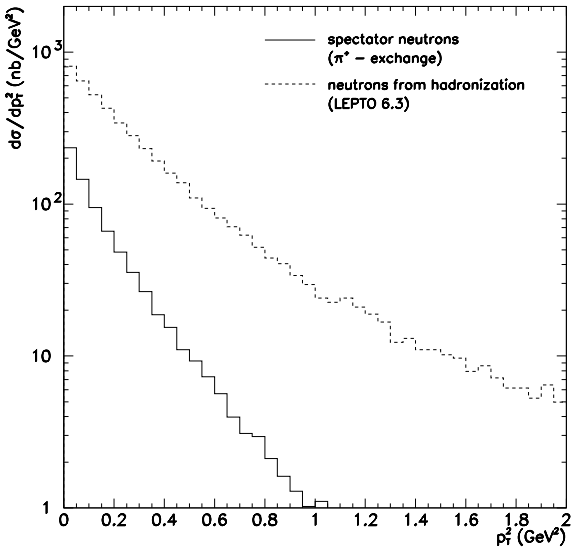

Fig. 3. Distribution in transverse momentum of neutrons from DIS on the proton (dashed histogram from LEPTO) and from DIS on a π^+ with a neutron as a spectator (solid histogram from POMPYT)

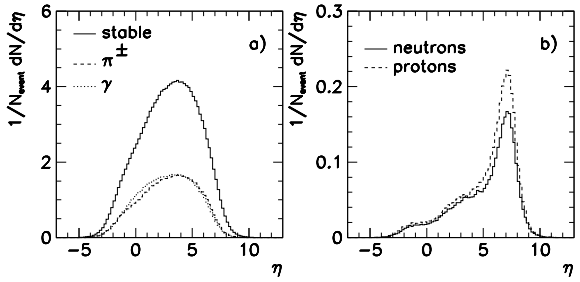

Fig. 4. Rapidity distributions of **(a)** all stable particles, charged pions and γ's and **(b)** protons and neutrons from DIS on the proton as obtained from LEPTO

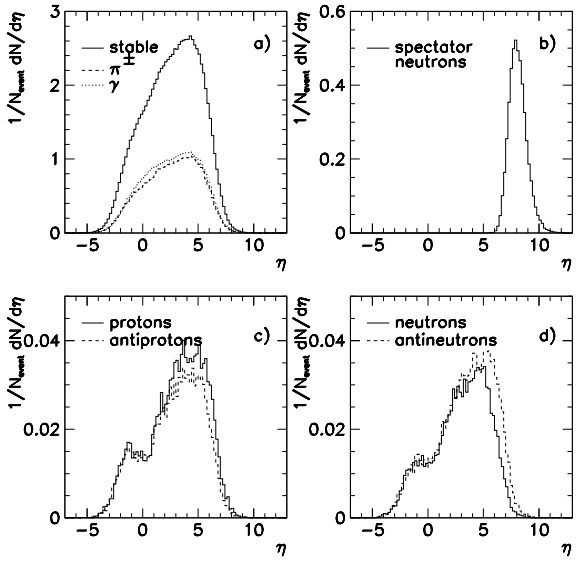

Fig. 5. Rapidity distributions of the specified particles produced in DIS on a π^+ (neutron spectator) as obtained from POMPYT

antiquark (quark) in addition to the valence quark and antiquark. A string is then stretched between the struck quark (antiquark) and a valence antiquark (quark), whereas the remaining valence quark (antiquark) forms a meson together with the spectator sea antiquark (quark).

For the results presented below we have made simulations corresponding to the HERA conditions, i.e. 26.7 GeV electrons on 820 GeV protons. The results for the above pion exchange mechanism are compared with normal DIS on the proton, which is simulated with LEPTO 6.3 [3] using the MRS(D-') parton distributions [31]. In all cases, events are simulated according to the cross section formulae and are constrained to be in the kinematical region $x > 10^{-5}$, $Q^2 > 4\,GeV^2$.

In Fig. 2 we show the resulting energy spectra of nucleons $(p, \bar{p}, n, \bar{n})$ in the lab frame of HERA. This is of direct interest for measurements in the leading proton spectrometer [18] and forward neutron calorimeter [17]. Neutrons from the pion exchange mechanism have large energies giving a spectrum with a broad peak around $E \approx 0.7E_{beam}$, i.e. around 500 GeV, whereas the corresponding spectrum from DIS on the proton decreases monotonically with increasing neutron energy. In the region of interest, say 400–700 GeV, the two processes have a similar absolute magnitude. An observable effect from DIS on a pion should therefore be possible.

While the energy distribution of primary Δ's is very similar to that of the direct neutron production [19], after the $\Delta \to n\pi$ decay the energy distribution of the secondary nucleons becomes peaked at smaller energies of about 400 GeV [32]. The two-step mechanism is, however, much less important for the production of neutrons. First of all the probability of the $\pi\Delta$ Fock states in the light-cone nucleon wave function is much smaller than the probability of the πN component: $P_{\pi\Delta} \approx 0.3P_{\pi N}$ [19]. Secondly, the isospin Clebsch-Gordan coefficients favour the decay of the Δ into the proton over the decay into the neutron channel with the proton/neutron branching ratio $\frac{7}{9} : \frac{2}{9}$. The analogous branching ratio for the direct component is $\frac{1}{3} : \frac{2}{3}$. All this imply that both the 1-step and 2-step mechanisms produce comparable amounts of protons. In contrast, the two–step mechanism produces about 10 times less neutrons than the 1-step mechanism. This means that in a first approximation the two-step process may be neglected for the spectrum of neutrons. Therefore we concentrate on the comparison of DIS on π^+, having a neutron as spectator, with standard DIS on the proton.

The calculated transverse momentum (p_T) distributions are shown in Fig. 3. As can be seen, the distribution of the spectator neutrons falls faster with increasing p_T^2 than that from standard DIS. It can be expected that the distribution of neutrons produced in the two-step process in Fig. 1b is less steep than those produced in the direct process in Fig. 1a. The higher overall level of DIS on the proton can be reduced by a cut in neutron energy, as is obvious from Fig. 2. Still, the difference in shape of the p_T^2-spectra in Fig. 3 is presumably too small to be exploited experimentally. A safe conclusion does, however, require further analysis including, e.g., finite angular acceptance of FNCAL.

To study other characteristics of events arising through DIS on a virtual pion and compare with standard DIS on the

proton, we consider spectra of different quantities normalized as

$$f(\kappa) \equiv \frac{1}{N_{event}} \frac{dN}{d\kappa} \ , \tag{9}$$

where κ can be any kinematical variable and N_{event} is the number of events. This gives emphasis to shapes irrespectively of normalisation and statistics (of data and Monte Carlo samples).

A quantity with especially nice transformation properties under longitudinal boosts is rapidity defined as

$$y = \frac{1}{2} ln \left(\frac{E + p_z}{E - p_z} \right) \ , \tag{10}$$

where E is the energy and p_z the longitudinal momentum along the proton beam axis. For massless particles this quantity is identical to the pseudo-rapidity defined by

$$\eta = -ln\, tan(\theta/2) \tag{11}$$

where θ is the angle of a particle with respect to the proton beam, i.e. $\eta > 0$ is the proton hemisphere in the HERA lab frame.

In Fig. 4 and 5 we show the pseudo-rapidity distributions of different particle species produced in DIS on the proton and DIS on a π^+, respectively. In Fig. 5a spectator neutrons are not included, but shown separately in Fig. 5b. For example, the size of the beam pipe hole in FCAL ($\theta = 1.5^0$), assures that in almost 100% of the spectator nucleons (proton/neutron) leaves the main ZEUS detector without any energy loss. As seen by comparing Fig. 4a and Fig. 5a the pseudo-rapidity spectra of $\pi^{\pm}$ and γ are rather similar in the two cases. The pseudo-rapidity spectrum of spectator neutrons (Fig. 5b) has a maximum at only a slightly higher value compared to the peak of neutrons from non-diffractive DIS on the proton (Fig. 4b). These predicted neutron distributions should be considered in the context of the pseudo-rapidity coverage of the forward neutron calorimeter. In general, the neutron acceptance is a complicated function of both polar and azimuthal angle. The ZEUS FNCAL geometry limits pseudo-rapidity coverage approximately to $7 \lesssim \eta \lesssim 10$. The Lund hadronization model predicts a small amount of nucleon-antinucleon pairs produced in DIS on the pion (Fig. 5cd).

The pseudo-rapidity variable is of particular interest in the context of large rapidity gap events. These have been defined by η_{max} giving, in each event, the maximum pseudo-rapidity where an energy deposition is observed. Based on our Monte Carlo simulated events using LEPTO and POMPYT we extract this η_{max}-variable and show its distribution in Fig. 6 for conventional non-diffractive DIS on the proton, DIS on an exchanged π^+ and diffractive DIS on a pomeron. Since our aim here is to demonstrate the genuine physics effects of the models, we have not included any experimental acceptance effects or rapidity gap requirements in this study. Doing this will severely distort the distributions at large η_{max} and, therefore, one cannot make direct comparisons with the available measured distributions. Thus, from this model study we find a shift of about one unit towards smaller η_{max} in case of DIS on the pion as compared to normal DIS. For $\eta_{max} \lesssim 6$, these two processes contribute about equally to the rate.

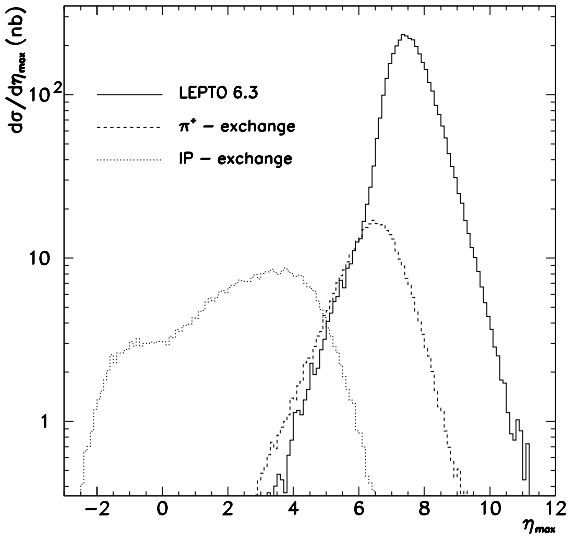

Fig. 6. Distribution of η_{max} (see text) in non-diffractive DIS on the proton (solid), in DIS on the virtual π^+ (dashed) and in DIS on the pomeron (dotted); pure physics of the models without experimental acceptance effects

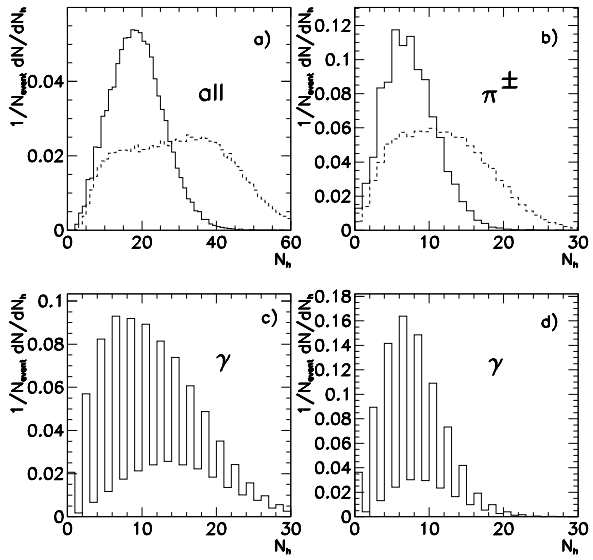

Fig. 7. Multiplicity distributions of **(a)** all stable particles, **(b)** charged pions from DIS on a π^+ (full curves) and DIS on a proton (dashed curves). In **(c)** γ's from DIS on the proton and **(d)** γ's from DIS on π^+

For the spectrum of η_{max} for DIS on the pomeron, we have taken a set of parameters which is usually called 'hard pomeron' in the literature. The pomeron is assumed to contain equal amounts of the light quarks, i.e. $u = \bar{u} = d = \bar{d}$, each with a density distribution

$$zq(z) = \frac{6}{4} z(1 - z) \ , \tag{12}$$

with the normalization chosen such that the parton distributions fulfill the momentum sum rule. The pomeron flux factor is here taken as the ratio of the single diffractive cross section and the pomeron-proton total cross section [33]

$$f_{I\!P/p}(x_{I\!P}, t) = \frac{d\sigma/dx_{I\!P}dt}{\sigma(I\!Pp \to X)} = \frac{1}{2.3} \frac{1}{x_{I\!P}} (3.19e^{8t} + 0.212e^{3t}) \ , \tag{13}$$

where the simple parameterization is obtained by fitting the numerator to single diffractive cross section and the denominator is taken as $\sigma(I\!Pp \to X) = 2.3\ mb$ obtained from a Regge analysis [34] of elastic and single diffractive scattering. The resulting η_{max} distribution from DIS on the pomeron is considerably different from the other two cases.

From Fig. 6 one may conclude that the pion–exchange induced DIS leads to events with intermediate size rapidity gaps rather than to those with large gaps. Nonetheless it is important to verify experimentally the effect of the pion exchange by, e.g., correlating η_{max} with fast forward neutrons measured in FNCAL (for technical details see [35]).

The flux factor given by (4) with a cut-off parameter of the vertex form factor extracted from the high-energy neutron production data [19] predicts that the pion carries, on average, a fraction 0.3 of the proton beam momentum [22]. This implies that as a first approximation the pion-induced DIS processes can be viewed as an electron scattering on the pion with effective energy $E_{eff} \approx 0.3 \cdot E_{beam}$. Because of the smaller energy of the pion one could expect smaller multiplicity of electron-pion DIS events in comparison to those for the electron-proton DIS. In Fig. 7 we compare the model predictions (without experimental acceptance effects) of the multiplicity spectra for DIS on the proton with those on π^+.

The multiplicities in DIS events on the pion is noticeably smaller than in DIS events on the proton; the average multiplicity is about 20 and 30, respectively. The dominant contribution to the multiplicity spectra comes from charged pions (11.6 on the proton vs. 7.5 on the π^+) and γ's (14.1 on the proton vs. 8.0 on π^+). The even-odd fluctuations of the multiplicity spectra of photons is not statistical, but caused mainly by the decay $\pi^0 \to \gamma\gamma$. Thus, as expected the multiplicity of standard DIS events is typically larger than in pion-induced DIS events. However, due to the large fluctuations in multiplicity and the overlap between the distributions for the two cases, as well as the distortions that limited experimental acceptance will create, it is not clear whether this difference can be used as a discriminator. This needs further considerations.

4 Conclusions

The concept of a pion cloud in the nucleon was recently found to be very useful [19, 25] in understanding the Gottfried sum rule violation observed by the New Muon Collaboration [8] and the Drell-Yan asymmetry measured recently in the NA51 Drell-Yan experiment at CERN [10]. In the present paper we have investigated several quantities in order to find useful observables which would help to verify this concept using deep inelastic electron-proton scattering at HERA. We have therefore analyzed the structure of deep inelastic events induced by the pion-exchange mechanism. In particular, we have studied distributions of final nucleons as well as rapidity and multiplicity spectra.

Most of the event characteristics do not provide a direct possibility to distinguish the events from DIS on a pion from the ordinary events with DIS on a proton. A clear difference is, however, found in the energy spectrum of outgoing neutrons. We find that the pion cloud model predicts an energy distribution of neutrons which substantially differs from the standard hadronization models. While the pion-exchange mechanism leads to an energy spectrum which peaks at an energy of about $0.7E_{beam}$, i.e. at about 500 GeV, the spectrum of neutrons produced in the standard hadronization process following DIS on the proton decreases monotonically with increasing neutron energy. This should facilitate to discriminate between the two processes, in particular since they have cross sections of similar magnitude in this energy region. Therefore, the experiments with forward neutron calorimeters should shed new light on the nucleon structure in terms of a pion content.

We have shown that the pion cloud induced mechanism practically does not contribute to the large rapidity gap events observed recently by the ZEUS and H1 collaborations [1, 2] and cannot be a severly competing mechanism for the pomeron exchange. The multiplicity of the pion cloud induced events is about 60-70% of that for standard hadronization on the proton, but given the large fluctuations it is not clear to what extent this difference can be exploited.

Our results on the pion exchange mechanism are more general than the detailed formulation of the pion cloud model. Since essentially the same pion flux factor is obtained in Regge phenomenology, our results may also be taken as a representation of Regge-based expectations.

In this study we have omitted experimental effects due to finite appertures, clustering effects in the main detector, finite energy thresholds, detector efficiencies, etc., which may distort the observed spectra. Many of them are quite important in order to understand and interpret the observed spectra and we plan a future study [36] of such effects.

References

1. ZEUS Collaboration, M.Derrick et al., Phys.Lett.B315 (1993) 481;
   ZEUS Collaboration, M.Derrick et al., Phys.Lett.B332 (1994) 228;
   ZEUS Collaboration, M.Derrick et al., Z.Phys.C68 (1995) 569.
2. H1 Collaboration, T.Ahmed et al., Nucl.Phys.B429 (1994) 477;
   H1 Collaboration, T.Ahmed et al., Phys.Lett.B348 (1995) 681.
3. G. Ingelman, LEPTO 6.3, unpublished manual, see also
   G.Ingelman, *LEPTO 6.1 – The Lund Monte Carlo for deep inelastic lepton–nucleon scattering*, Proc. of the DESY Workshop 'Physics at HERA. Ed. W.Buchmüller and G.Ingelman. Hamburg (1991) 1366
4. B.Andersson, G.Gustafson, G.Ingelman and T.Sjöstrand, Phys.Rep.97 (1983) 31
5. K.Werner and P.Koch, Z.Phys.C47 (1990) 215,255.
6. W. Buchmüller, A. Hebecker, Phys. Lett. B355 (1995) 573
   A. Edin, G. Ingelman, J. Rathsman, Phys. Lett. B366 (1996) 371
7. EMC Collaboration, J.Ashman et al., Nucl. Phys. B328 (1989) 1.
   SMC Collaboration, D.Adams et al., Phys. Lett. B329 (1994) 399.
8. NMC Collaboration, P.Amaudruz et al., Phys.Rev.Lett.66 (1991) 2712.
9. A.D.Martin, W.J.Stirling and R.G.Roberts, Phys.Rev.D50 (1994) 6734.
10. A.Baldit et al., Phys.Lett.B332 (1994) 244.
11. E.M.Henley and G.A.Miller, Phys.Lett.B251 (1990) 453;
    S.Kumano, Phys.Rev. D43 (1991) 59;
    A.Signal, A.W.Schreiber and A.W.Thomas, Mod.Phys.Lett. A6 (1991) 271;
    W-Y.P.Hwang, J.Speth and G.E.Brown, Z.Phys.A339 (1991) 383;
    V.R.Zoller, Z.Phys. C53 (1992) 443;
    A.Szczurek and J.Speth, Nucl.Phys. A555 (1993) 249;
    A.Szczurek, H.Holtmann, Acta Phys.Pol. B24 (1993) 1833;
    A.Szczurek, J.Speth and G.T.Garvey, Nucl.Phys. A570 (1994) 765.

12. M.Lusignoli and Y.Srivastava, Nucl.Phys. B138 (1978) 151;
M.Lusignoli, P.Pistili and F.Rapuano, Nucl.Phys. B155 (1979) 394;
C.L.Korpa, A.E.L.Dieperink and O.Scholten, Z.Phys. A343 (1992) 461;
G.D.Bosveld, A.E.L.Dieperink and O.Scholten, Phys.Rev. C45 (1992) 2616.
13. A.Szczurek, G.D.Bosveld, A.E.L.Dieperink, Groningen preprint KVI-1096 (1994), Nucl.Phys. A595 (1995) 307.
14. G.D.Bosveld, A.E.L.Dieperink and A.G.Tenner, Phys.Rev. C49 (1994) 2379.
15. G.Levman and K.Furutani, Virtual pion scattering at HERA, ZEUS note 92-107 (1992)
G.Levman and K.Furutani, A forward Neutron Calorimeter for ZEUS, DESY-PRC 93-08 (1993).
16. H.Holtmann, G.Levman, N.N.Nikolaev, A.Szczurek and J.Speth, Phys.Lett.B338 (1994) 363.
17. S.Bhadra et al., Nucl.Instr. and Meth. A354(1995)479.
18. The ZEUS detector, status report, 1993, DESY.
19. H.Holtmann, A.Szczurek and J.Speth, Jülich preprint KFA-IKP(TH)-25 (1994), Nucl.Phys. A569 (1996) 631.
20. R.G.E.Timmermans, Th.A.Rijken and J.J. de Swart, Phys.Lett. B257 (1991) 227.
21. B.Holzenkamp, K.Holinde and J.Speth, Nucl.Phys. A500 (1989) 485.
22. H.Holtmann, A.Szczurek and J.Speth, Jülich preprint KFA-IKP(TH)-33 (1993)
23. M.V.Terent'ev, Sov.J.Nucl.Phys.24 (1976) 106;
H.J.Weber, Ann.Phys.177 (1987) 38;
C.-R. Ji, P.L.Chung and S.R.Cotanch, Phys.Rev.D45 (1992) 4214;
T.Huang, B.-Q.Ma and Q.-X.Shen, Phys.Rev.D49 (1994) 1490.
24. J.D.Sullivan, Phys.Rev.D5 (1972) 1732.
25. H.Holtmann, N.N.Nikolaev, J.Speth and A.Szczurek, Jülich preprint KFA-IKP(TH)-14 (1994), Z.Phys.A353 (1996) 411.
A.Szczurek, M.Ericson, H.Holtmann and J.Speth, Jülich preprint KFA-IKP(TH)-05 (1995), Nucl.Phys.A596 (1996) 397.
26. P. Bruni, G. Ingelman, POMPYT 2.3 – A Monte Carlo to simulate diffractive hard scattering processes, unpublished program manual
27. T. Sjöstrand, PYTHIA 5.7 and JETSET 7.4, CERN-TH.7112/93 and Comp. Phys. Comm. 82 (1994) 74
28. M.Glück, E.Reya and A.Vogt, Z.Phys.C53 (1992) 651.
29. J.Badier et al., Z.Phys.C18 (1983) 281.
30. P.J.Sutton, A.D.Martin, R.G.Roberts and W.J.Stirling, Phys.Rev.D45 (1992) 2349.
31. A.D.Martin, R.G.Roberts and W.J.Stirling, Phys.Lett.B306 (1993) 145.
32. H.Holtmann, N.N.Nikolaev, A.Szczurek, J.Speth and B.G.Zakharov, Jülich preprint KFA-IKP(TH)-06 (1995), Z.Phys. C69 (1996) 297.
33. G.Ingelman and P.Schlein, Phys.Lett.152B (1985) 256.
34. E.L.Berger, J.C.Collins, D.E.Soper and G.Sterman, Nucl.Phys.B286 (1987) 704.
35. M.Birkič, Ph.D. dissertation, DESY internal report, DESY F35D-95-10, 1995.
36. M.Przybycień and A.Szczurek, work in progress.